Proceedings of the 37th Chinese Control Conference
July 25-27, 2018, Wuhan, China

Motion blurred image restoration based on flight control system

Ran Zhao[1], Dongliang Liu[1,2], Feng Qu[1], Xu Zhang[1]

1. Academy of Automation, Hangzhou Dianzi University, Hangzhou 310018
E-mail: 15958018984@163.com

2. Wolong Electric CO., LTD, Shangyu 312300, China
E-mail: liudl@hdu.edu.cn

Abstract: In recent years, the applications of Aerial UAV are more and more extensive. The aerial system is subject to the impact of the relative movement, posture changes and the atmosphere, which results in low clarity of the captured image. Based on the image blur phenomenon caused by UAV flight, a function is introduced as its coefficient in Lucy-Richardson (LR) image restoration algorithm, which could effectively protect edge details of the image. The results of image quality evaluation show that the improved LR algorithm can effectively suppress the noise in the image and improve the clarity of the image.

Key Words: Flight control system, image restoration, Motion blur, LR algorithm, Evaluation of Image quality

1 Introduction

In the UAV aerial photographing process, the clarity of image suffers from the relative movement between camera and scenery, that is, the motion blurred image is generated. Nowadays, the restoration of motion blurred images is widely used in the fields of military, traffic, medical images, industrial control and so on. Therefore, it is of great practical significance to study the restoration of fuzzy images.

The restoration technique of motion blurred images means that the fuzzy image is the input, and a clear image closer to the original image is the output. The inverse filtering method (Deconvolution method) proposed in the middle of the 60s is widely used in digital image restoration, but the inverse filtering method is very sensitive to noise interference. When the noise is large, its recovery effect is very poor. In 1967,Helstrom improved the inverse filtering method, and proposed Wiener filtering method, which made the restored image and original image have the smallest mean square error, which meant good resistance to noise[1]. Then Pratt and Habibi studied the effectiveness of the Wiener filtering calculation and improved the computing speed[2, 3], but it is necessary to know the signal-to-noise ratio to obtain the best restoration effect of the degraded image, which is difficult to be realized in reality. In 1970s, Richardson and Lucy put forward a deconvolution method based on probability statistics Bayes theory, also known as Richardson-Lucy (R-L) algorithm[4,5], which has been widely used in the restoration of blurred images. Although the Lucy-Richardson algorithm (LR algorithm) can achieve an ideal restoration effect, the edge ringing effect usually occurs near the restored image boundary, besides, human vision is very sensitive to it. To this end, the researchers put forward many improvements. For example, multi channel blind restoration[6] can achieve better recovery effect, but it takes a long time. Iterative adaptive method[7] reduces the number of iterations and improves the peak signal-to-noise ratio, which has a certain restoration effect on blurred images. But the effect of edge restoration is still not ideal. The regularization method[8] has good image restoration results, but it could not restore the image edge well, so it is not very good in visual angle.

In this paper, an improved method is proposed on the basis of the Lucy-Richardson algorithm, that is, adding the coefficient term to the iterative formula to restrain the restored image. The analysis of the experimental results shows that the improved algorithm proposed in this paper can not only restore the edge of aerial image very well, but also make the restored image avoid the influence of noise to the maximum.

2 Fundamental

2.1 Dynamic modeling of four rotor unmanned aircraft under external disturbance

Angular Displacement Equation of Quad-rotor in Navigational Coordinate System:

$$\begin{aligned} \ddot{\theta} &= l(F_1 - F_2 + F_3 - F_4 - k_1\dot{\theta})/I_x \\ \ddot{\vartheta} &= l(F_1 + F_2 - F_3 - F_4 - k_2\dot{\vartheta})/I_y \\ \ddot{\varphi} &= l(F_1 - F_2 - F_3 + F_4 - k_3\dot{\varphi})/I_z \end{aligned} \tag{1}$$

l is the distance between the center of each propeller and the center of gravity of the four rotor aircraft; I is the moment of inertia on each axis; $k_i(i=1,2,3)$ indicates air resistance coefficient. Due to the lower relative speed of Quad-rotor UAV, this factor can be neglected.

Quad-rotor UAV can change the lift of each rotor by adjusting the speed of the four rotor, so as to realize the attitude change of the UAV. The input quad-rotor UAV flight control system can be expressed as:

$$\begin{aligned} u_1 &= F_1 - F_2 + F_3 - F_4 \\ u_2 &= F_1 + F_2 - F_3 - F_4 \\ u_3 &= F_1 - F_2 - F_3 + F_4 \end{aligned} \tag{2}$$

Under the action of outside wind field, the total lift generated by each rotor of the UAV is:

* This work is supported by National Nature Science Foundation of China under Grant 51277048 and Major Science and Technology Projects of Zhejiang Province under Grant 2015C01SA620003.

$$F_Z = F_R - F_T = 2\rho S V_d \hat{V} - k_f \rho \Omega^2 = 2\rho S V_d V_w \quad (3)$$

$$F_Z = 2\rho S V_d (\hat{V} - V_d) = 2\rho S V_d V_w$$

V_d is the flow induced velocity of the rotor rotation, and V_w is the induction velocity of the external flow field.

We use the changes in the rotational speed of each rotor blade on behalf of the disturbance of the external wind farm on the quad-rotor UAV. The induction velocity of the external wind field is set to V_{w1}. The force of the blade subjected to the external wind field is F_{Z1}. The current induction speed of the rotor is V_{d1}.

$$F_{Z1} = 2\rho S V_{d1} V_{w1} \quad (4)$$

The total lift force produced by the UAV rotor is:

$$\begin{aligned} F_R &= F_T + F_Z \\ &= 2\rho S V_{d1}^2 + 2\rho S V_{d1} \\ &= 2\rho S V_{d1}(V_{d1} + V_{w1}) \end{aligned} \quad (5)$$

According to the blade lift force is proportional to the blade speed:

$$F_R = F_T + F_Z = k_f \Omega^2 + 2\rho S V_{d1} V_{w1} \quad (6)$$

$$k_f \Omega^2 = 2\rho S V_{d1}^2 \quad (7)$$

Thus, it can be concluded that the induction speed of rotor is:

$$V_{d1} = \sqrt{\frac{k_f \Omega^2}{2\rho S}} \quad (8)$$

Substitute (8) into (6):

$$F_R = F_T + F_Z = k_f \Omega^2 + 2\rho S \sqrt{\frac{k_f \Omega^2}{2\rho S}} V_{w1} \quad (9)$$

It can be concluded that under the condition of stable blade size and air density, the total lift of the blades is determined by the induced speed and rotor speed in the external wind field.

Substituting (9) into (1) and (2):

$$\begin{aligned} \ddot{\theta} &= l(F_{R1} - F_{R2} + F_{R3} - F_{R4} - k_1 \dot{\theta}) / I_x \\ \ddot{\vartheta} &= l(F_{R1} + F_{R2} - F_{R3} - F_{R4} - k_2 \dot{\vartheta}) / I_y \\ \ddot{\varphi} &= l(F_{R1} - F_{R2} - F_{R3} + F_{R4} - k_3 \dot{\varphi}) / I_z \end{aligned} \quad (10)$$

$$\begin{aligned} u_{R1} &= F_{R1} - F_{R2} + F_{R3} - F_{R4} \\ u_{R2} &= F_{R1} + F_{R2} - F_{R3} - F_{R4} \\ u_{R3} &= F_{R1} - F_{R2} - F_{R3} + F_{R4} \end{aligned} \quad (11)$$

F_{R1}、F_{R2}、F_{R3}、F_{R4} represent the total lift of four blades under the disturbance of the outside wind field; u_{R1}、u_{R2}、u_{R3} represent the rolling force, the pitching force and the yaw force of the four blades under the disturbance of the external wind field, respectively.

The flight control system model of quad-rotor UAV under the disturbance of the outside wind field:

$$\begin{aligned} \ddot{\theta} &= l u_{R1} / I_x \\ \ddot{\vartheta} &= l u_{R2} / I_y \\ \ddot{\varphi} &= l u_{R3} / I_z \end{aligned} \quad (12)$$

The system controls the lift of the propeller directly mounted on the drive motor of the four rotor by controlling the speed of the driving motor. The speed of the drive motor is accomplished by adjusting the driving voltage. The relationship between the driving voltage and the lift of the rotor is a linear.

2.2 Degradation Model of UAV Aerial Photographs

Many reasons can cause image degradation to form motion blur. Usually they can be divided into two categories: deterministic factors and random factors. The deterministic factors include improper focusing of imaging system or relative motion between camera and target object, and atmospheric turbulence effect such as aerial photography when exposed for a long time. Random factors mainly refer to noise pollution in the process of signal transmission, digitalization and recording. The relationship between the degraded image and the clear image in the motion blurred image degradation model can be expressed as the following mathematical expressions in the airspace and the frequency domain:

$$\begin{aligned} g(x,y) &= h(x,y) * f(x,y) + n(x,y) \\ G(u,v) &= H(u,v)F(u,v) + N(u,v) \end{aligned} \quad (13)$$

$g(x,y)$ is motion blurred image; $f(x,y)$ is an implicit clear image, $h(x,y)$ is the spatial domain representation of point spread functions; $n(x,y)$ is additive noise; $*$ is convolution operator. The restoration of motion blurred image is to find the best estimation of the original image so that it is as close as possible to the original image. That is the problem of minimization:

$$\min \left\| f(x,y) - f'(x,y) \right\|^2 \quad (14)$$

$\|\bullet\|$ represents L_2 norm.

3 Improved LR image restoration algorithm

3.1 L-R image restoration algorithm

Lucy-Richardson algorithm is one of the most widely used techniques for image restoration. It is an iterative method. According to the Bayes formula:

$$\begin{aligned} f(x,y) &= \arg\max p(f,h \mid g) \\ &\propto p(g \mid f,h) p(f) p(h) \end{aligned} \quad (15)$$

$p(f,h \mid g)$ represents the estimation of the original image; $p(g,f \mid h)$ represents likelihood; $p(h)$ represents point spread function; $p(f)$ represents original image;

$p(g)$ represents degenerate image. The noise model of the Lucy-Richardson algorithm conforms to the Poisson distribution, and the clear image of the model can be expressed as:

$$p(g \mid f,h) = \prod_{(x,y)} \frac{(f*h)(x,y)^{g(x,y)} \exp\{-(f*h)(x,y)\}}{g(x,y)!} \quad (16)$$

For the sake of simplicity, the following formula will omit (x,y), then $f^{'}(x,y)$ can be obtained by energy minimization:

$$f^{'} = \arg\min E(f) \quad (17)$$

Because of $h(x,y)$ meets $\sum\sum h(x,y)=1$, the iterative estimation equation of LR is:

$$f^{t+1} = f^{t}[h^{*} \otimes \frac{g}{f^{t} \otimes h}]$$
$$h^{t+1} = h^{t}[\frac{g}{h^{n} \otimes f^{n}} \otimes f^{*}] \quad (18)$$

$h^{*}(x,y) = h^{t}(-x,-y)$, $f^{*}(x,y) = f^{t}$, t represents the number of iterations.

3.2 Improved LR image restoration algorithm

In this paper, an improved LR image restoration algorithm is proposed and a model is constructed:

$$f^{t+1} = \frac{1}{1+p(x,y)} f^{t}[h^{*} \otimes \frac{g}{f^{t} \otimes h}] \quad (19)$$

$p(x,y)$ is defined as:

$$p(x,y) = \frac{1}{1+\left|\nabla G_{\sigma} * f^{0}\right|^{2}} \quad (20)$$

f^{0} is the initial image; G_{σ} is Gauss filter, $\sigma > 0$; ∇ is the gradient.

This algorithm is analyzed as follows:

①A Gauss filter is used to preprocess the image $f^{0} = g$ before the initial iteration to suppress the false edges formed by the noise.

②According to the correlation between the value of $p(x,y)$ and pretreatment image gradient, we can know $0 < p(x,y) < 1$. At the edge of the image, because of $\left|\nabla G_{\sigma} * f^{0}\right| \to \infty$, the function of type (9) is equivalent to the use of a low pass filter after the restoration of the LR algorithm for A in order to reduce the high frequency part to achieve a smooth transition between high and low frequencies. In a smooth area, $\left|\nabla G_{\sigma} * f^{0}\right| \to 0$. The smoothing area uses LR algorithm to recover. In this paper, the improved LR algorithm can keep the edge of the image and further restrain the noise existing in the image, thereby effectively improving the image clarity.

4 Quality evaluation of restoration image

4.1 Peak signal to noise ratio

$$MSE = \frac{\sum_{i=1}^{M}\sum_{j=1}^{N}[f(i,j)-g(i,j)]^{2}}{M \times N} \quad (21)$$

4.2 mean square error

$$PSNR = 10\lg\{\frac{255 \times 255}{\frac{1}{M \times N}\sum_{i=1}^{M}\sum_{j=1}^{N}[f(i,j)-g(i,j)]^{2}}\} \quad (22)$$

4.3 Structural similarity

Compared with other methods, the quality evaluation index of structural similarity is more consistent with the human visual system. Structural similarity is a method based on structural information to measure the degree of similarity between the original signal and the processing signal.

The quality evaluation index of structural similarity is:

(1) Gray contrast index:

$$l(x,y) = \frac{2u_{x}u_{y} + C_{1}}{u_{x}^{2} + u_{y}^{2} + C_{1}} \quad (23)$$

The constant $C_{1} = (K_{1}L)^{2}$ is designed to avoid the instability produced when $u_{x}^{2} + u_{y}^{2}$ is near 0. L is the maximum gray level, the constant K_{1} is far less than 1, usually 0.01.

(2) Contrast index:

$$c(x,y) = \frac{2\sigma_{x}\sigma_{y} + C_{2}}{\sigma_{x}^{2} + \sigma_{y}^{2} + C_{2}} \quad (24)$$

The constant $C_{2} = (K_{2}L)^{2}$ is designed to avoid the instability produced when $\sigma_{x}^{2} + \sigma_{y}^{2}$ is near 0. The constant K_{2} is far less than 1, usually 0.03.

(3) Structural contrast index:

$$s(x,y) = \frac{\sigma_{xy}^{2} + C_{3}}{\sigma_{x}\sigma_{y} + C_{3}} \quad (25)$$

C_{3} is a proper selection of constants. The synthesis of these three indicators can be obtained:

$$SSIM(x,y) = l(x,y)^{\alpha} c(x,y)^{\beta} s(x,y)^{\gamma} \quad (26)$$

For all the corresponding points of the two image, the value of $SSIM(x,y)$ is obtained, and then the value of $SSIM(X,Y)$ is obtained on average. The greater the structural similarity between the two images, the more similar the two images are.

5 Simulation and experimental results

The experimental environment: i5 processor, 8GB memory, dual core CPU, MatlabR2011a. In order to enhance the reliability of the experiment, a comparative experiment on two types of images is made. Two sets of pictures (College, Dorm) are processed respectively by Wiener filter, LR algorithm and the improved LR algorithm. Finally, through three different methods of image quality evaluation,

the advantages and disadvantages of several algorithms of moving blurred image are compared, and a detailed analysis is made.

5.1 Simulation results

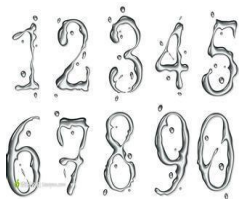

Fig. 1: Original Image

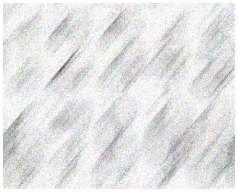

Fig. 2: Blurred Image

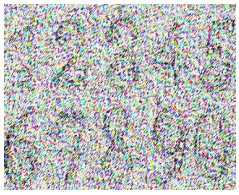

Fig. 3: Wiener filtering restoration

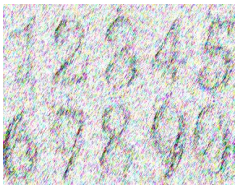

Fig. 4: L-R restoration

Fig. 5: improved L-R restoration

It can be seen that the Wiener filtering in Figure 3 can basically restore the outline of the figure, but it is not clear. In Figure 4, the L-R algorithm can recover the number better. The algorithm can better recover the details of images in this paper. It is obvious that the algorithm is better than the L-R algorithm in recovering numbers 3 and 9.

5.2 Comparison of image quality evaluation

Table 1: Quality evaluation of 'College' restoration

Comparison of quality evaluation parameters			
	PSNR	MSE	SSIM
wiener filtering	19.8617	595.0536	0.83732
L-R algorithm	23.5883	99.2917	0.99543
improved L-R	26.5618	86.7791	0.99581

From the data analysis of Table 1, it is found that the improved L-R algorithm can not only get higher PSNR value, but also make the value of K closer to 1, and has more easily distinguishable details. This shows that the algorithm has better visual effect on the restoration of motion blurred images, and the clarity of the recovered image is higher.

Table 2: Quality evaluation of 'Dorm' restoration

Comparison of quality evaluation parameters			
	PSNR	MSE	SSIM
wiener filtering	23.6152	1025.39	0.8675
L-R algorithm	26.7646	531.8663	0.9162
improved L-R	28.3663	147.5643	0.9938

According to the data analysis of Table 2, we can get that the improved L-R algorithm can completely retain the details of the image, and effectively suppress the ringing effect of the image edge. The restoration effect of motion blurred image is better.

5.3 Experimental results

Fig. 6: Original College

Fig. 7: Blurred College

Fig. 8: Wiener filtering restoration

Fig. 9: L-R restoration

Fig. 10: improved L-R restoration

It can be concluded that Wiener filtering algorithm and Lucy-Richardson algorithm have better image restoration results, but the results of restored images are basically affected by the number of iterations, and the number of iterations is very difficult to determine in actual operation.

The comparison between Figure 9 and Figure 10 shows that the proposed algorithm can reduce the ringing effect near the image boundary better. Especially for the blurred image with larger contrast, Figure 10 shows that our algorithm can better construct the edge of the image.

Fig. 11: Original Dorm

Fig. 12: Blurred Dorm

Fig. 13: Wiener filtering restoration

Fig. 14: L-R restoration

Fig. 15: improved L-R restoration

It can be seen from the comparative analysis that the fuzzy image contains the pixels in the saturated region and the impact noise. It can be seen clearly that the improved L-R algorithm has rich details and clearer visual effects on the restoration of motion blurred images.

6 Conclusion

In this paper, the problem of image definition based on flight control system is mainly studied. Motion blur phenomenon often appears in UAV aerial images. In order to restore the blurred image better, the improved L-R algorithm is adopted in this paper. The algorithm uses the L-R method to restore the image in the smooth region, and adds the coefficient at the edge to preserve the details of the image. Through the simulation experiment, it is proved that the improved L-R algorithm can eliminate the ringing effect of the image edge more effectively than the traditional L-R algorithm. Applying this algorithm to the flight control system, the motion blur phenomenon of the aerial image is well restrained.

References

[1] C W Helstrom. Image restoration by the method of least squares [J]. Opt. Soc. Amer. 1967, 57(3): 297-303.

[2] W K Pratt, Generalized Wiener filter computation techniques[C].IEEE,TransComputers,1972,c-21(7):636-641.

[3] A Habibi. Fast suboptimal Wiener filtering of markov processes[R]. Los Angeles: University of Southern California, USCIPI Report 530, 1974: 75-80.

[4] W H Richardson. Bayesian-based iterative method of image restoration [J]. JOSA, 1972, 62: 55-59.

[5] L B Lucy. An iterative technique for the rectification of observed distributions [J]. The Astronomical Journal, 1974, 79(6):745-754.

[6] Zou L. Multi - channel image restoration algorithm based on LLT model (in Chinese) [D]. Hunan University, 2012.

[7] Zhang Xinming, Cheng Jinfeng, Kang Qiang, Wang Xia. Iterative Adaptive Weight Means Filtering for Image Denoising [J]. Computer Application, 11:1-9, 2017.

[8] Wu Xianjin, Wang Runsheng. Regularized Image Restoration Based on Edge Recovery and Artifact Removal [J]. Journal of Electronics & Information Technology, 04:577-581, 2006.

[9] Ting-Fa Xu, Peng Zhao. Interlaced scan CCD image motion deblur for space-variant motion blurs [J].Optik - International Journal for Light and Electron Optics,2010,122(8):.

[10] Xu Bin; Wang Danwei; Zhang Youmin. DOB-Based Neural Control of Flexible Hypersonic Flight Vehicle Considering Wind Effects, IEEE Transactions on Industrial Electronics, 64(11):8676-8685, 2017.

[11] Lin, Yucong; Saripalli, Srikanth. Sampling-Based Path Planning for UAV Collision Avoidance, IEEE Transactions on Intelligent Transportation Systems, 18(11):3179-3192, 2017.

[12] Xu, Xiangyu; Pan, Jinshan; Zhang, Yu-Jin. Motion Blur Kernel Estimation via Deep Learning, IEEE Transactions on Image Processing, 27(1): 194-205, 2017.

[13] Jenie, Yazdi I.; van Kampen, Erik-Jan; Ellerbroek, Joost;Taxonomy of Conflict Detection and Resolution Approaches for Unmanned Aerial Vehicle in an Integrated Airspace[J].IEEE TRANSACTIONS ON INTELLIGENT TRANSPORTATION SYSTEMS,2017,18(3):558-567.

[14] Zaugg, Evan C.; Long, David G.Theory and Application of Motion Compensation for LFM-CW SAR[J].IEEE TRANSACTIONS ON GEOSCIENCE AND REMOTE SENSING ,2008,46(10):2990-2998.

[15] Jafar, Adnan; Fasih-UR-Rehman, Syed; Fazal-UR-Rehman, Syed.A Robust H-infinity Control for Unmanned Aerial Vehicle against Atmospheric Turbulence[J].International Conference on Robotics and Artificial Intelligence,2016:87-92.

[16] Lee, Ho-Joon; Ahn, Han-Woong; Lee, Jae-Kwang.Newly Proposed Hybrid Type Mutli-DOF Operation Motor for Multi-Copter UAV Systems[C].IEEE Energy Conversion Congress and Exposition,2015: 2782-2790.H. Poor, An Introduction to Signal Detection and Estimation. New York: Springer-Verlag, 1985, chapter 4.

[17] D. Cheng, On logic-based intelligent systems, in Proceedings of 5th International Conference on Control and Automation, 2005: 71–75.

[18] D. Cheng, R. Ortega, and E. Panteley, On port controlled hamiltonian systems, in *Advanced Robust and Adaptive Control — Theory and Applications*, D. Cheng, Y. Sun, T. Shen, and H. Ohmori, Eds. Beijing: Tsinghua University Press.